Tetrahedron 66 (2010) 1689–1698

Contents lists available at ScienceDirect

Tetrahedron

journal homepage: www.elsevier.com/locate/tet

Anion recognition through hydrogen bonding by adamantane-dipyrromethane receptors

Marija Alešković [a], Nikola Basarić [a], Kata Mlinarić-Majerski [a,*], Krešimir Molčanov [b], Biserka Kojić-Prodić [b], Manoj K. Kesharwani [c], Bishwajit Ganguly [c,*]

[a] Department of Organic Chemistry and Biochemistry, Ruđer Bošković Institute, Bijenička cesta 54, 10000 Zagreb, Croatia
[b] Department of Physical Chemistry, Ruđer Bošković Institute, Bijenička cesta 54, 10000 Zagreb, Croatia
[c] Central Salt & Marine Chemicals Research Institute (CSIR), Bhavnagar-364 002, Gujarat, India

ARTICLE INFO

Article history:
Received 17 September 2009
Received in revised form 16 November 2009
Accepted 4 January 2010
Available online 11 January 2010

ABSTRACT

Adamantane-dipyrromethane (AdD) receptors [di(pyrrole-2-yl)methyladamantane (**1**), 2,2-di(pyrrole-2-yl)adamantane (**2**), 1,3-bis[di(pyrrole-2-yl)methyl]adamantane (**3**), 2,2,6,6-tetra(pyrrole-2-yl)adamantane (**4**)] form complexes with F^-, Cl^-, Br^-, AcO^-, NO_3^-, HSO_4^-, and $H_2PO_4^-$. The association constants of the complexes were determined by ^1H NMR titrations, whereas the geometries of complexes **1**·$\mathbf{F^-}$ (2:1), **2**·$\mathbf{F^-}$ (2:1), **2**·$\mathbf{Cl^-}$ (2:1), **2**·$\mathbf{AcO^-}$ (2:1), and **4**·$\mathbf{F^-}$ (1:1) were determined by X-ray structural analysis. The most stable complexes are of 2:1 stoichiometry with F^- and AcO^-. The stability constants are in accordance with the anion basicity and the ability of AdD receptors to place the hydrogen bonding donor groups in a tetrahedral fashion around anions. The binding energies of the complexes between receptors **1**–**4** and F^- anion are calculated using quantum chemical methods. The calculated results show that the solvent polarity is important for the complexation of fluoride ion with AdD receptors **1**–**4**.

1. Introduction

In recent years, anion complexation has attracted attention and become an intensively studied area of supramolecular chemistry.[1] Considerable interest has been focused to produce a variety of new selective anion receptors[2] for different applications such as: fluorescent and chromogenic anion sensors,[3] ion selective electrodes,[4] phase-transfer catalysis,[5] or templates in supramolecular synthesis.[6] In biological systems, anions have important roles in signalling, and transport events and are becoming a subject of interest in medicine. These demands initiated the tremendous growth in the field of supramolecular chemistry of anions and there is a continuing challenge to design new selective receptors for detection, transport or extraction of anionic species.

One of the important interactions between receptor and anion is related to hydrogen bonding. Pyrrole derivatives can act as anion complexing agents due to their acidic NH protons, which can bind anions forming hydrogen bonds. Polypyrrolic macrocycles[7] (calixpyrroles, porphyrins) were the first examples of these receptors. Substitution of the pyrrole moiety with the additional hydrogen bond donating groups, such as amide[8] or guanidinium,[9] lead to the development of better hosts, potent in complexing anions with higher selectivity and affinity. On the other hand, dipyrrolylquinoxalines are simple receptors bearing only two pyrrole units, which bind inorganic anions with appreciably high binding constants.[10] These findings motivated us to investigate whether the dipyrromethane moiety with two NH sites, can function as an anionic receptor. Dipyrromethanes are simple molecules that can be easily synthesized and purified,[11] and therefore, could be readily available for the anion binding essays.

The representative examples of the anionic receptors containing rigid spacers are the urea and the thiourea derivatives of norbornene.[12] Recently we prepared a series of substituted dipyrromethane derivatives bearing rigid adamantane subunits.[13] Incorporation of the rigid bulky adamantane unit was expected to decrease rotational mobility of the pyrroles and thus increase the stability of the complexes with anions. Furthermore, the lipophilicity of the adamantane could be a great advantage in the applicability of the dipyrromethanes as anion transfer agents in the extraction studies. We also reported that adamantane-dipyrromethanes (AdD) receptors bind the following anions: F^-, Cl^-, Br^-, HSO_4^- and $H_2PO_4^-$.[14]

In this paper we report further investigation of the anion binding ability of the AdD receptors including two additional oxo-anions with planar Y-shaped geometry, acetate and nitrate.

* Corresponding authors. Tel.: +385 1 4680 196; fax: +385 1 4680 195.
E-mail addresses: majerski@irb.hr (K. Mlinarić-Majerski), ganguly@csmcri.org (B. Ganguly).

0040-4020/$ – see front matter © 2010 Elsevier Ltd. All rights reserved.
doi:10.1016/j.tet.2010.01.018

Particular emphasis is given to understanding the reasons for the formation of the observed unexpected complex stoichiometries. Therefore, we investigated the crystal structures of the AdD complexes with anions. Finally, we performed a theoretical study of the anion binding by quantum chemical calculations. These results should contribute to better understanding of the intermolecular interactions, and particularly, use of the multiple hydrogen-bonding sites, that give rise to the formation of supramolecules characterised by specific geometries. In addition, the information from the crystal packing may appoint implementations of these adamantane-derivatives as preorganized receptors in coordination chemistry of anions, and possibly, in the field of crystal engineering.[15]

2. Results and discussion

2.1. Synthesis and association constants

Adamantane-dipyrromethane receptors **1**–**4** (Chart 1) were prepared by following the published procedure for the synthesis of phenyldipyrromethane **5**.[11]

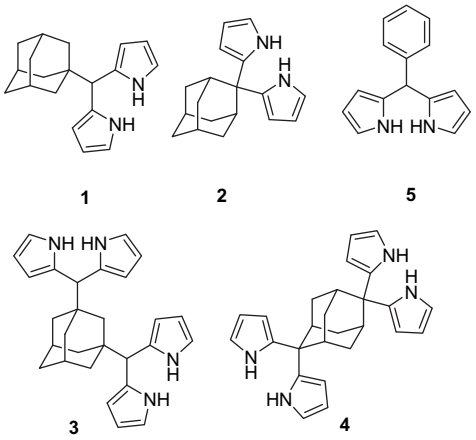

1 2 5

3 4

Chart 1.

The AdD derivatives **1**–**4** were prepared from pyrrole and the corresponding adamantane carbonyl derivatives: adamantane-1-carbaldehyde (**6**), adamantan-2-one (**7**), adamantane-1,3-dicarbaldehyde (**8**) and adamantan-2,6-dione (**9**), in 51%, 29%, 37% and 15% yield, respectively, (e.g., Scheme 1).

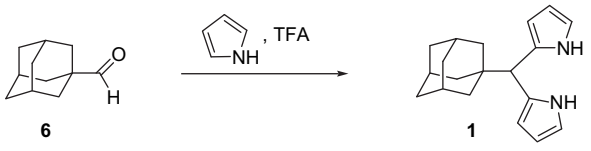

6 1

Scheme 1.

We have reported binding of AdD receptors **1**–**4** with three spherical halogenides (F^-, Cl^- and Br^-) and two oxo-anions with tetrahedral geometry (HSO_4^- and $H_2PO_4^-$).[14] We showed that AdD receptors bind Cl^-, Br^-, HSO_4^- and $H_2PO_4^-$, forming 1:1 complexes characterised by moderate association constants ($\sim 10^2\ M^{-1}$). Furthermore, AdD formed very stable complexes with F^- (association constants in the range 10^3–$10^5\ M^{-2}$) characterised by the stoichiometries (AdD–F^-) 2:1 for derivatives **1**–**3**, or 1:1 and 1:2 for AdD **4**. In order to investigate the influence of the geometry of the anion on the stability constant of the AdD complexes, the binding study with two additional planar anions (AcO^- and NO_3^-) was performed. As previously described,[14] the binding of the anions was investigated by ^1H NMR titrations with tetrabutylammonium salts. The titrations were performed at rt by recording spectra in $CDCl_3$ solution. Although ion pairing could occur in $CDCl_3$,[16] this solvent was chosen for titrations to get comparable results with our previous report.[14] In addition, the titration results obtained in that solvent wherein stabilization of the charges by solvation is not as pronounced as in polar solvents, should principally be more comparable with the calculations results performed for the gas phase (vide infra). For **4**, because of its insolubility, the spectra were recorded in DMSO-d_6.

The changes observed in the spectra upon addition of AcO^- to the solution of AdD derivatives can be demonstrated on the examples of AdD **2** and **3**. The addition of 2.5 equiv of the AcO^- to the $CDCl_3$ solution of **2**, shifted downfield the NH signal from the initial value of δ 7.8 to 12.3 ppm. In addition, changes of the chemical shifts of the pyrrole C3-H and C4-H protons (upfield shift of 0.25 ppm) were observed. Chemical shifts of the bridgehead adamantane protons changed $\sim$0.4 ppm to lower magnetic field. Similar features in the spectra were observed during the titrations of **3** with AcO^-. However, the changes were more pronounced than with **2**. Already a small quantity of acetate (0.125 equiv) had a dramatic effect on the spectra. The signal of the free pyrrole NH at δ 7.9 disappeared and the new, broadened one appeared at 8.8 ppm. With the addition of 2 equiv of AcO^- the NH signal moved to 11.5 ppm. Besides changes in the chemical shift of the NH signal, smaller effects were seen on the chemical shifts of the pyrrole CH and the dipyrromethane *meso* protons. Similar, albeit smaller, changes were observed upon titration of other AdD receptors with AcO^-, as well as on titration with NO_3^-. Although additions of NO_3^- to the solution of **1** and **2** showed pronounced changes of the NH chemical shift, the association constants (vide infra) revealed very low stability of the nitrate complexes.

The binding stoichiometries and the association constants with AcO^- and NO_3^- were estimated using the EQNMR program.[17] The constants are compiled in Table 1, together with the association constants with F^-, Cl^-, Br^-, HSO_4^-, $H_2PO_4^-$. In addition, Job plot[18] analyses were used to reveal the formation of the complexes with specific stoichiometry depending on the anion used. The results of the binding are compared with those obtained with dipyrromethane having the phenyl substituent in the *meso* position (**5**). The fitting of the titration results with AcO^- for **1**, **2**, and **3** indicated the presence of two complexed species in the solution, complexes 1:1 and 2:1, whereas for **4** and **5** the presence of only 1:1 complexes was indicated with the association constants being lower by two orders of magnitude. It is interesting to compare these results with the binding of other ions. Generally, except for **4**, 2:1 stoichiometry of binding was observed with F^- and AcO^-, and the association constants were high. On the other hand, the other anions formed 1:1 complexes with much lower association constants. The logical presumption that arises from this finding is that two ligand molecules are needed, and four hydrogen bonds should be formed with the anion to create the stable complex. Furthermore, the stability of the complex could be related to the anion basicity, rather than its geometry. However, the geometry of the AdD receptor plays an important role in the binding. For an example, AdD **3** has in principle two binding sites, but the dipyrromethane arms may adopt a conformation wherein the complex with an anion would be formed with four hydrogen bonds. In AdD **4**, two dipyrromethane moieties are further apart, but as suggested from the values of the association constants, the binding is cooperative. That is, when the first F^- is bound, providing sufficiently high F^- concentration, the second F^- is being bound with the higher association constant by an order of magnitude. Although it is known that in the presence of the basic F^- a deprotonation of the pyrrole could take place,[16b,19] it is not the case for receptor **4**. During the titration with F^-, the

Table 1
The association constants of the complexes of dipyrromethanes **1–5** with anions determined by ^{1}H NMR titration[a]

Compound.	F^{-}[c, d]	Cl^{-}[d]	Br^{-}[d]	HSO_4^{-}[d]	$H_2PO_4^{-}$[d]	AcO^{-}	NO_3^{-}
1	$(1\pm0.1)\times10^4$ (2:1)	80±10 (1:1)	22±4 (1:1)	65±3 (1:1)	150±10 (1:1)	110±7 (1:1) and $(2.5\pm0.6)\times10^3$ (2:1)	50±4 (1.1)
2	$(4.4\pm0.1)\times10^3$ (2:1)	68±6 (1:1)	38±3 (1:1)	22±2 (1:1)	182±9 (1:1)	766±86 (1:1) and $(2.2\pm0.5)\times10^4$ (2:1)	63±9 (1.1)
3	$(4.8\pm0.5)\times10^5$ (2:1); $\sim1\times10^4$ (2:1)[g] and $\sim1\times10^3$ (1:1)[g]	ND[f]	ND[f]	$(1.4\pm0.8)\times10^3$ (1:1)	ND[e,f]	261±70 (1:1) and $(9.7\pm0.8)\times10^5$ (2:1)	ND[f]
4[b]	150±40 (1:1) and $(3.3\pm0.7)\times10^3$ (1:2)	ND[h]	ND[h]	ND[h]	74±20 (1:1)	26±3 (1:1)	ND[h]
5	170±20 (1:1) and $(2.3\pm0.2)\times10^4$ (2:1)	22±2 (1:1)	4.8±0.8 (1:1)	6 ± 1 (1:1)	32±2 (1:1)	31±3 (1:1)	ND[f]

[a] The titrations were performed in $CDCl_3$ solution unless stated otherwise. The anions were added as tetrabutylammonium salts. The association constants were determined by fitting the dependence of the chemical shift of the NH signal ($\Delta\delta$) to the anion concentration, using EQNMR program. The complexes were formed in 1:1 stoichiometry giving K_{11} ($mol^{-1}\,dm^3$), 2:1 giving K_{21} ($mol^{-2}\,dm^6$) and 1:2 (**4**×2F^-) giving K_{12} ($mol^{-2}\,dm^6$).
[b] The titration was performed in DMSO-d_6 because of insolubility in $CDCl_3$.
[c] Content of water was at<5 wt %.
[d] Results are from Ref. 14.
[e] Titration was performed in CD_3CN because of precipitation during the titration in $CDCl_3$.
[f] Titration data could not be fitted to 1:1 or 1:2 stoichiometries or their combination.
[g] The titration of **3** was also performed in DMSO-d_6; however the data could not be fitted well; indicating the presence of the mixture of 1:1 and 2:1 complexes. The observed lower binding constant is in accord with the polarity of used solvent.[16]
[h] No binding observed.

signal of the pyrrole NH protons constantly shifted downfield from 10.09 to 13.37 ppm, and no change in the peak intensity was observed upon addition of 2.5 equiv (see Supplementary data p. S2). To find answers to the above mentioned different topologies we turn to the crystal structures of the complexes and the theoretical studies.

2.2. Crystal structures

Single crystals of the complexes: **1**·F^- (2:1), **2**·F^- (2:1), **2**·Cl^- (2:1), **2**·AcO^- (2:1), **4**·F^- (1:1) and receptor **2** were obtained by slow evaporation of different solvent mixtures (see Experimental section). In the crystal structure of **2** (see Supplementary data, Fig. 9S), the molecule adopts a conformation with two pyrrolyl moieties pointing in opposite directions (vide infra, conformation **2a**, Fig. 7). On the other hand, in the crystal structures of the anion complexes, the pyrroles adopt a conformation wherein NH are pointing to the same side forming hydrogen bonds with anions (Figs. 1–6, Table 2).

In all crystal structures, the adamantyl moieties have C_1 symmetry and are therefore located in general positions. Two adamantyl molecules per asymmetric unit are found in **2**·F^-, **2**·AcO^- and **2**·Cl^-. As each receptor molecule of **2** provides two proton donor groups, two receptor molecules are required to stabilize the anion with four hydrogen bonds (Figs. 2,5 and 6; the asymmetric unit of the crystal comprises two molecules). The anions and tetrabutylammonium counterions are also located in general positions, except in the complex of **1**·F^- (2:1), in which both cation and anion have C_2 symmetry. Regarding the geometrical orientation of the adamantyl moieties in the complexes (vide infra, Charts 2 and 3) in **2**·F^- (2:1) they are *syn*-oriented, whereas in the other complexes the adamantanes are in the *anti*-orientation.

The crystal structures of the complexes are particularly informative regarding the topology of the complexes. They reveal: (a) overall conformations of the receptor moieties that define a cavity suitable for accommodation of particular anion, and (b) the orientations of proton donor groups that should be accessible to the anion for hydrogen bonding. In the investigated complexes, the anions are acceptors of four hydrogen bonds (Table 2). It is interesting to correlate the association constants of the complexes (Table 1) with the hydrogen bond length. However, for the stability

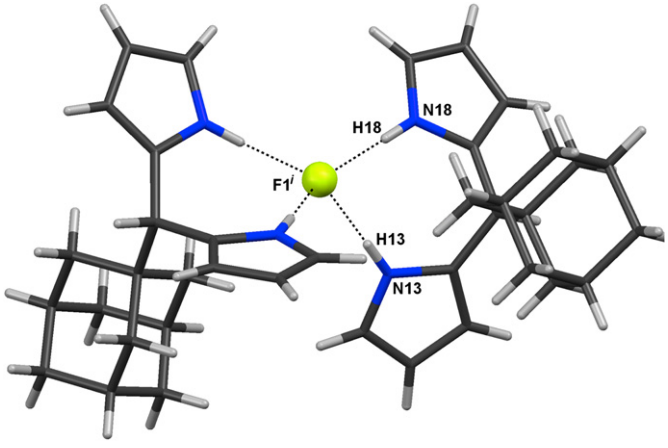

Figure 1. Distorted tetrahedral environment about the fluoride ion (located on the crystallographic two-fold axes) in the crystal structure of **1**·F^-. The fluoride anion has been depicted as a sphere of an arbitrary radius. Symmetry operator: (i) x, y, 1+z.

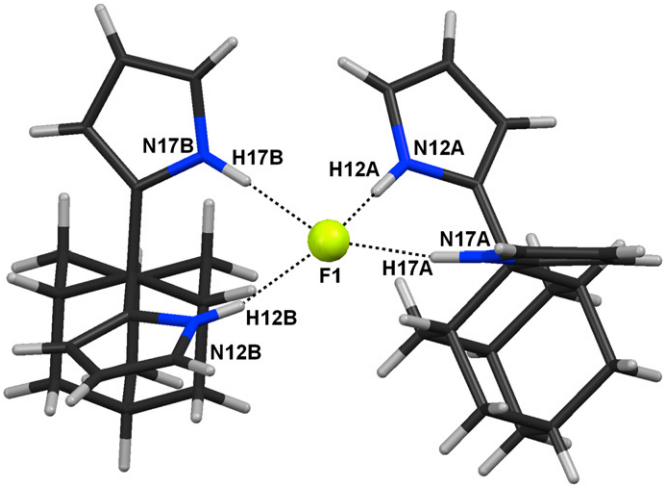

Figure 2. Distorted tetrahedral environment about the fluoride ion in the crystal structure of **2**·F^-. The fluoride anion has been depicted as a sphere of an arbitrary radius.

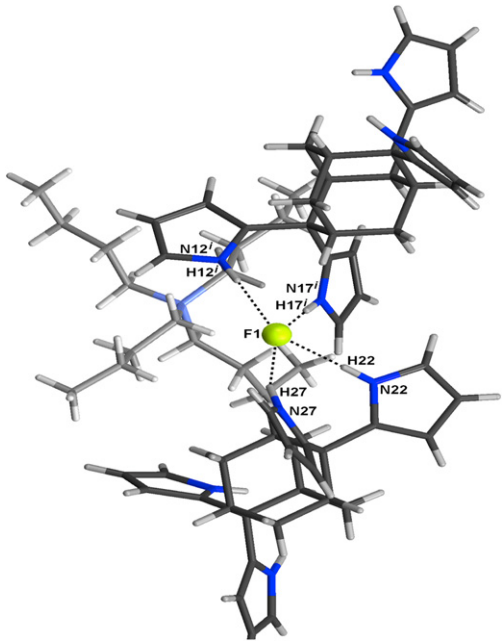

Figure 3. Distorted tetrahedral environment about the fluoride anion in the crystal structure of **4**·$\mathbf{F}^-$. A tetrabutylammonium cation is nearby, although no close contacts could be observed. The fluoride anion has been depicted as a sphere of an arbitrary radius. Symmetry operators: (i) x, 2−y, $^1/_2$ +z.

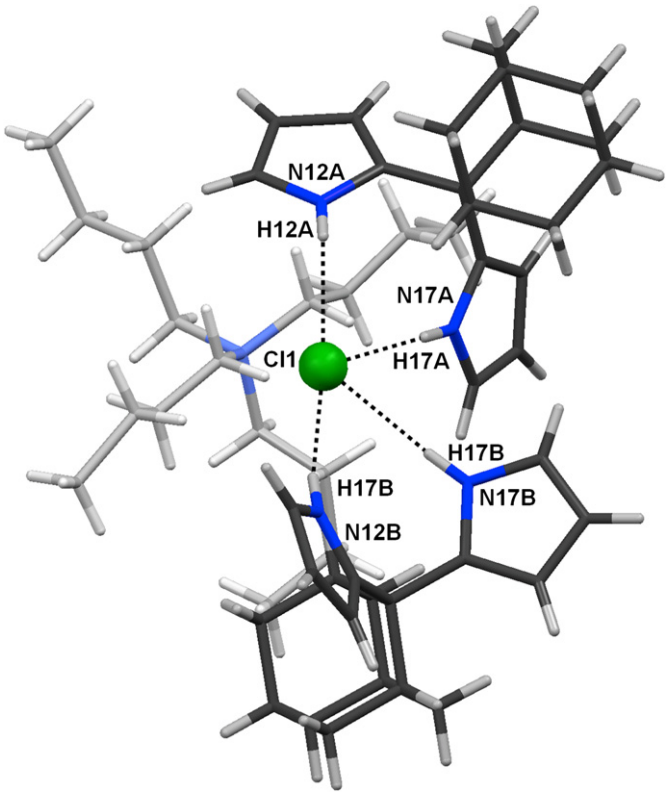

Figure 5. Environment of the chloride anion in the crystal structure of **2**·$\mathbf{Cl}^-$. The four hydrogen bonds are roughly coplanar, forming a half-coordination sphere, while the other half of the anion makes weak contacts with a tetrabutylammonium cation (Cl···N and Cl···H distances are longer than sums of van der Waals radii). The chloride anion has been depicted as a sphere of an arbitrary radius.

of the complexes, the spatial arrangements of the proton donor groups are essential for optimal hydrogen bonding with anions. The small F^- anion fits well into a cavity between two dipyrromethane moieties and has a distorted (flattened) tetrahedral environment (Figs. 1–4). It is also the strongest acceptor of hydrogen bonds among the studied complexes. The larger, more polarisable Cl^- and AcO^-, cannot fit into the cavity between two dipyrromethane moieties. Therefore, the spatial arrangement is different; four almost coplanar hydrogen bonds are located on the one side of the anion (Fig. 5 and 6). The AdD pyrrolyl NH donors form a half-sphere around the anion; the other half is surrounded either by a tetrabutylammonium cation (compensating the charge of the chloride anion, Fig. 5) or hydrophobic parts of the adamantyl moieties (surrounding the methyl group of the acetate anion, Fig. 6). The hydrogen bonding geometry is typical of NH···Cl^- and NH···O bonds[20] (Table 2).

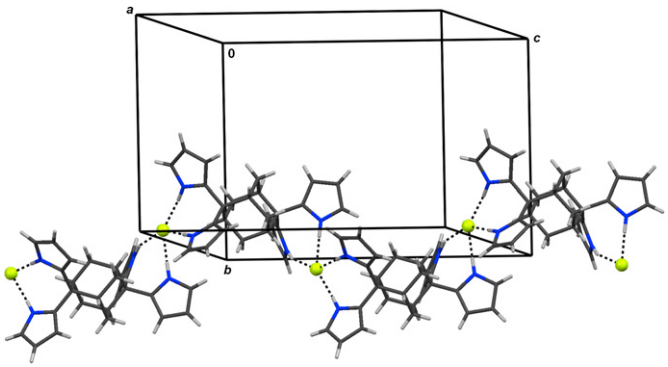

Figure 4. Infinite hydrogen bonded chains of alternating adamantyl donors and fluoride anions in the structure of **4**·$\mathbf{F}^-$. The chains are parallel to [001] and are generated by a c glide plane. The fluoride anions have been depicted as spheres of an arbitrary radii.

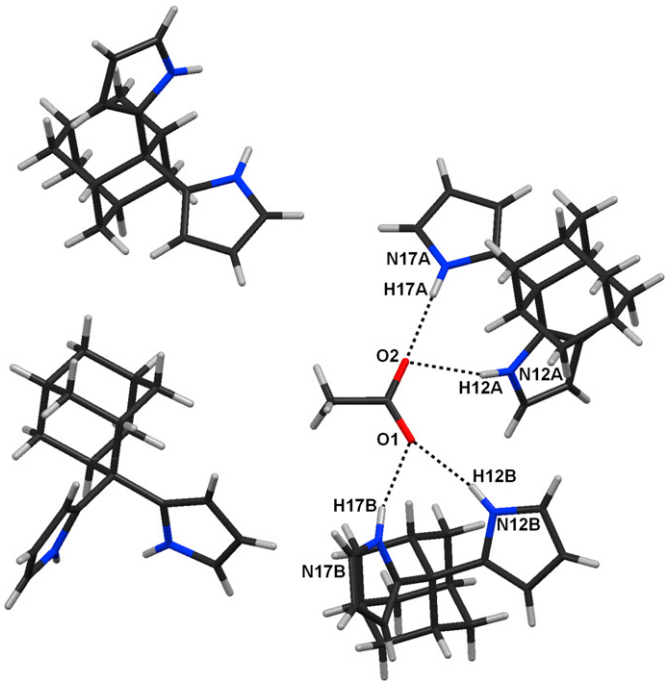

Figure 6. Environment of the acetate anion in the crystal structure of **2**·$\mathbf{AcO}^-$. The four hydrogen bonds are roughly coplanar, forming a half-coordination sphere around the carboxylic group, while the methyl group is surrounded by hydrophobic parts of two molecules of **2**.

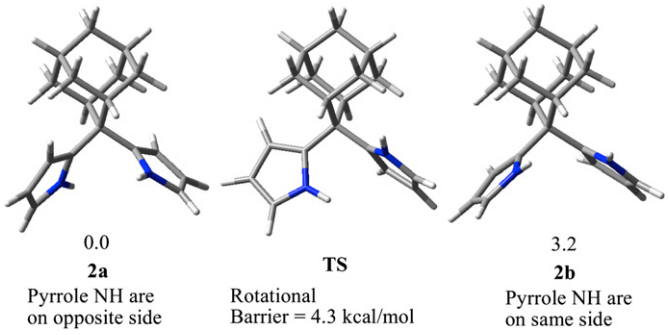

Figure 7. Semi-empirical PM3 optimized geometries and relative energies (kcal/mol) for two possible conformer of **2** (**2a** and **2b**) and transition state (**TS**) with rotational barrier. (Grey: carbon; blue: nitrogen; white: hydrogen).

The stability constants of the complexes with Cl^- are lower by several orders of magnitude compared with the fluoride complexes. The F^- coordination in **4**·$\mathbf{F}^-$ (1:1) can be regarded as a transition state between a planar and a flattened tetrahedral environment. The nearby located tetrabuytlammonium cation uses a space available in the vicinity of the complex (Fig. 3). The donor molecules in **4**·$\mathbf{F}^-$ (1:1) are capable of hydrogen bonding to two different anions, creating infinite zig–zag hydrogen bonded chains, which extend in the direction [001] and are generated by a c glide plane operation (Fig. 4). The hydrogen bonds between receptor molecules and anions reveal the same motif described by the graph-set symbol $2R_2^1(7)$.[21]

Investigation of the Cambridge Structural Database (CSD)[22] indicates that in the solid state the pyrrole moiety is ubiquitous complexing agent for Cl^- (62 structures), whereas there is a paucity of structural data on pyrrole complexes with F^- (7 structures) and AcO^- (3 structures). In half of the Cl^- complexes, the Cl^- anion is acceptor of four hydrogen bonds from four pyrrole NH groups, which are usually coplanar forming a half-sphere similar to one in Figure 5. There are also 17 structures with a three-coordinated Cl^-, where the donors are roughly coplanar, and usually, in a half-sphere fashion. Among the reported complexes with Cl^-, most host molecules are calixpyrroles or extended porphyrins, and therefore are not directly related to our structures. However, Sessler et al. reported Cl^- complexes with dipyrromethanes[23] and Gale et al. reported coordination of a pyrrolic amide derivative.[24]

In the reported crystal structures with F^-, binding of the anion is most often accomplished with four hydrogen bonds, but three hydrogen bonds (pyrrole NH and two amide NH),[25] and five hydrogen bonds surrounding (with pyrrole NH) have also been reported.[26] The most common motif in four-coordinated complexes is the structure of calixpyrrole wherein F^- sits on a cone formed by four pyrrole NH. Furthermore, Sessler also reported one dipyrromethane complex with F^-.[7g] The geometry of that complex is very similar to **1**·$\mathbf{F}^-$ (Fig. 1), however, the anion is surrounded by four, almost coplanar hydrogen bonds, whereas in **1**·$\mathbf{F}^-$ a distorted tetrahedral environment allows a stronger complexation. In the

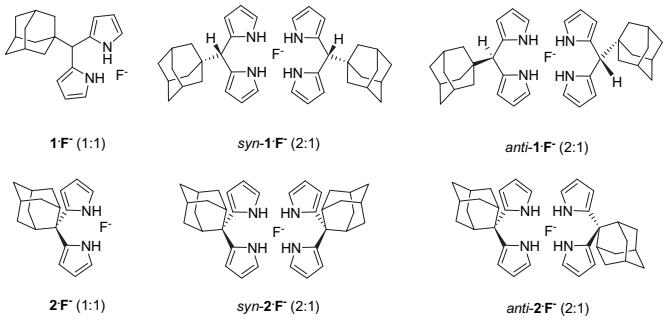

Chart 2.

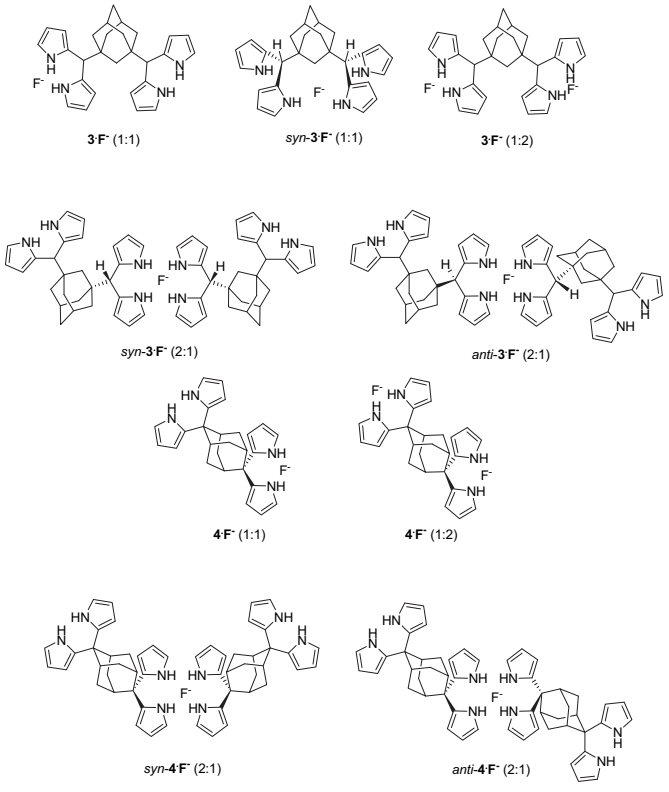

Chart 3.

Table 2
Geometric parameters of the hydrogen bonds in crystal structures presented in this paper

	d(*D*-H)/Å	d(H···*A*)/Å	d(*D*···*A*)/Å	(*D*-H···*A*)/°	Symm. op. on *A*
1·$\mathbf{F}^-$					
N13–H13···F1	0.86	1.85	2.710 (2)	176	*x*, *y*, 1+*z*
N18–H18···F1	0.86	1.86	2.716 (2)	176	*x*, *y*, 1+*z*
2·$\mathbf{Cl}^-$					
N12A–H12A···Cl1	0.86	2.53	3.374 (2)	168	*x*, *y*, *z*
N12B–H12B···Cl1	0.86	2.53	3.342 (2)	159	*x*, *y*, *z*
N17A–H17A···Cl1	0.86	2.42	3.280 (2)	173	*x*, *y*, *z*
N17B–H17B···Cl1	0.86	2.43	2.368 (2)	166	*x*, *y*, *z*
C1A–H1A···Cl1	0.98	2.80	3.761 (3)	168	*x*, *y*, *z*
2·$\mathbf{F}^-$					
N12A–H12A···F1	0.86	1.99	2.822 (4)	161	*x*, *y*, *z*
N12B–H12B···F1	0.86	1.96	2.799 (4)	164	2−*x*, 2−*y*,−*z*
N17A–H17A···F1	0.86	1.86	2.716 (4)	171	*x*, *y*, *z*
N17B–H17B···F1	0.86	1.84	2.696 (4)	175	2−*x*, 2−*y*,−*z*
C3B–H3B···F1	0.98	2.38	3.310 (5)	158	2−*x*, 2−*y*,−*z*
2·$\mathbf{AcO}^-$					
N12A–H12A···O2	0.86	2.18	2.996 (6)	158	*x*, *y*, *z*
N12B–H12B···O1	0.86	2.08	2.898 (5)	159	*x*, *y*, *z*
N17A–H17A···O2	0.86	1.94	2.781 (6)	166	*x*, *y*, *z*
N17B–H17B···O1	0.86	1.99	2.823 (6)	162	*x*, *y*, *z*
C3A–H3A···O2	0.98	2.60	3.524 (6)	157	*x*, *y*, *z*
N3B–H3B···O1	0.98	2.54	3.464 (5)	157	*x*, *y*, *z*
4·$\mathbf{F}^-$					
N12–H12···F1	0.86	1.91	2.729 (4)	159	*x*, 2−*y*, −1/2+*z*
N17–H17···F1	0.86	1.98	2.839 (5)	178	*x*, 2−*y*, −1/2+*z*
N22–H22···F1	0.86	1.84	2.700 (4)	179	*x*, *y*, *z*
N27–H27···F1	0.86	1.98	2.792 (5)	156	*x*, *y*, *z*
C1–H1···F1	0.98	2.54	3.458 (4)	156	*x*, 2−*y*, −1/2+*z*
C7–H7···F1	0.98	2.54	3.454 (4)	155	*x*, *y*, *z*

reported structures with AcO^-, the anion is surrounded by three[27] or four hydrogen bonds[28] and sits on the cone of the calixpyrrole, or forms two hydrogen bonds with an amide H-atom and one with the pyrrole NH in the complex with amidopyrrole.[29]

In the crystal packing, the discrete hydrogen bonded receptor-anion units [or 1 D in the structure of **4**·F^- (1:1)] do not display hydrophobic/hydrophilic layered organisation typical of amphiphilic adamantyl compounds. Rather, isolated hydrophilic complex-units and chains [in the complex of **4**·F^- (1:1)] are embedded into a hydrophobic, nonpolar matrix of adamantyl moieties and tetrabutylammonium cations. Therefore, 3D packing is achieved only through weak dispersion interactions. This explains the difficulties in growth of the crystals, their small size, softness, and poor diffraction (see Supplementary data). The only exception is ligand **2**, which has a layered structure typical of amphiphilic compounds, despite a lack of hydrogen bonds.

2.3. Computational results

Although crystal structures give the best information regarding the geometry of the complexes, this geometry is restricted to the solid state, and is not necessarily the same in the dynamic solution system. To examine the binding energies of receptors **1**–**4** with the fluoride ion, quantum chemical calculations were performed. Considering the fact that the sizes of receptors are relatively larger in these cases, initially semi-empirical PM3 calculations[30] were employed to examine the binding energies for AdD receptors **1** and **2** with F^- ion. However, the reliability of semi-empirical PM3 methods was evaluated with additional calculations for **1** and **2** towards complex formation with fluoride ion at B3LYP/6-31+G* level of theory.[31] The calculated binding energies for **1**·F^- (1:1) and **2**·F^- (1:1) were found to be comparable at both B3LYP/6-31+G* and PM3 levels (Table 3). After establishing the efficacy of PM3 method, larger systems **3** and **4** were also computed at this PM3 level. For more accurate predictions of binding energies employing PM3 calculated geometries, single point calculations were performed using ONIOM method at (B3LYP/6-31+G*:PM3) level.[32]

The ONIOM calculations were performed by dividing the complex of **1**–**4** with fluoride ion in two layers: pyrrole rings and fluoride ion was treated with B3LYP/6-31+G* (high layer) and other atoms were treated with semi-empirical PM3 model (low layer). The connecting atoms between the pyrrole rings and adamantane moiety were also treated at B3LYP level (see Supplementary data Fig. 14S). The Charts 2 and 3 show the possible geometries of the complexes with F^- for the receptors **1**–**4**. The calculated binding energies using PM3 and ONIOM (B3LYP/6-31+G*:PM3)//RHF/PM3 for these complexes are given in Table 4.

The binding energies calculated with both methods reveal that **1**·F^- (2:1) is energetically preferred over **1**·F^- (1:1). This is in agreement with the experimental reports (vide supra). In addition, two geometries of the **1**·F^- (2:1) complex can be formed, with adamantyl moieties oriented *syn*- or *anti*-. The complexation of fluoride ion with *syn*-**1**·F^- (2:1) and *anti*-**1**·F^- (2:1) is comparable in binding energy (Table 4). However, in the crystal structure, the molecules adopt the conformation with two adamantyl moieties in the *anti*-orientation.

For AdD **2**, two conformers were calculated, with pyrrole nitrogens pointing to opposite sides (**2a**, Fig. 7) and with pyrrole nitrogens pointing to the same side (**2b**, Fig. 7). Both conformers were optimized by PM3 method and it was found that **2a** is more stable than **2b**. The computational results are in a good agreement with the observed crystal structure, wherein the two pyrrole rings are pointing to the opposite sides. On the other hand, the complexation of **2b** with F^- is more preferred than that of **2a** in both 1:1 and 2:1 ratio (see Table 4, and Supplementary data Fig. 15S). The same orientation of the pyrrole rings was also seen in the crystal structure of the complex **2**·F^- (Fig. 2). Thus, in the complexation process, the pyrrole ring rotates to adopt the conformation capable of forming two hydrogen bonds with the anion. The barrier for the rotation of the pyrrole ring from **2a** to **2b** is calculated to be 4.3 kcal/mol, (Fig. 7). However, the calculated energy of the binding in 2:1 complexes, wherein four hydrogen bonds are formed (Table 4), far exceeds the value needed for the rotation of the pyrrole ring. The calculation data also showed that binding of AdD **2** with F^- in a 2:1 ratio is energetically more favoured compared with the 1:1 complex. In addition, two conformations of the complex are possible with dipyrromethane moieties oriented *syn* or *anti* (Chart 2, Fig. 8), and the former one is more stable (3 kcal/mol) at both levels of theory. These results also corroborate the observed crystal structure of **2**·F^- (vide supra).

For AdD **3**, four different conformers were optimized and **3a** was found to be the lowest in energy (Fig. 9). Therefore, further calculations were performed using the **3a** conformer. To examine the complexation process of **3** with F^-, calculations were performed with 1:1, 1:2 and 2:1 ratios. For 1:1 complexation two geometries were optimized: (a) **3**·F^- (1:1) in which only two pyrrole N–H were interacting with F^-, and (b) *syn*-**3**·F^- (1:1) in which all four pyrrole N–H interact with F^-, forming a basket-like structure (Fig. 10). Calculated binding energies suggest that F^- binds more strongly in *syn*-**3**·F^- (1:1) than in **3**·F^- (1:1) (Table 4). In **3**·F^- (1:2), two fluoride ions were interacting with one AdD **3** molecule showing complexation of each F^-, with two pyrrole NH. For the 2:1 complex with F^-, binding energies were calculated for two possible orientations, *syn*-**3**·F^- (2:1) and *anti*-**3**·F^- (2:1). In both geometries of

Table 3
B3LYP/6-31+G* and PM3 (in parenthesis) calculated binding energies (kcal/mol) for **1** and **2** interacting with fluoride ion in 1:1 ratio

Complex	Binding Energy (kcal/mol)
1·F^- (1:1)	−57.3 (−60.8)
2·F^- (1:1)	−57.4 (−57.5)

Table 4
Semi-empirical PM3 and ONIOM (B3LYP/6-31+G*:PM3)//RHF/PM3 (in parenthesis) calculated binding energies (kcal/mol) for receptors **1**–**4** interacting with fluoride ion in different ratio

AdD·F^-	(1:1)	*anti*-(2:1)	*syn*-(2:1)	(1:2)
1·F^-	−60.8	−95.9	−96.8	—
	(−56.2)	(−88.7)	(−88.1)	
2·F^-	−57.5 [−47.1][a]	−89.1	−92.1 [−78.5][b]	—
	(−52.5) [(−43.8)][a]	(−81.1)	(−84.0) [(−74.6)][b]	
3·F^-	−57.3 [−81.6][c]	−92.3	−87.9	−78.3
	(−54.1) [(−74.8)][c]	(−86.7)	(−78.7)	(−69.5)
4·F^-	−86.1	−100.4	−97.1	−81.3
	(−65.4)	(−97.4)	(−87.7)	(−75.1)

[a] Nitrogen of the pyrrole rings are *anti* to each other and only one NH group interacted with the fluoride ion.
[b] Nitrogen of both pyrrole rings are *anti* to each other in both receptor molecules and only one NH group of each molecule interacts with F^-.
[c] Fluoride interacted with all four NH, forming a basket like geometry *syn*-**3**·F^- (1:1).

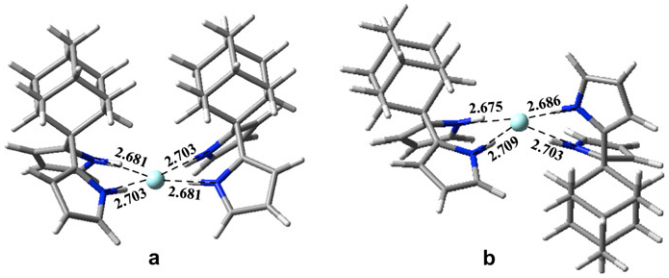

Figure 8. Semi-empirical PM3 optimized geometry of 2:1 complexes of *syn*-**2**·F^- (a) and *anti*-**2**·F^- (b) showing pyrrole nitrogen-fluoride distances (Å).

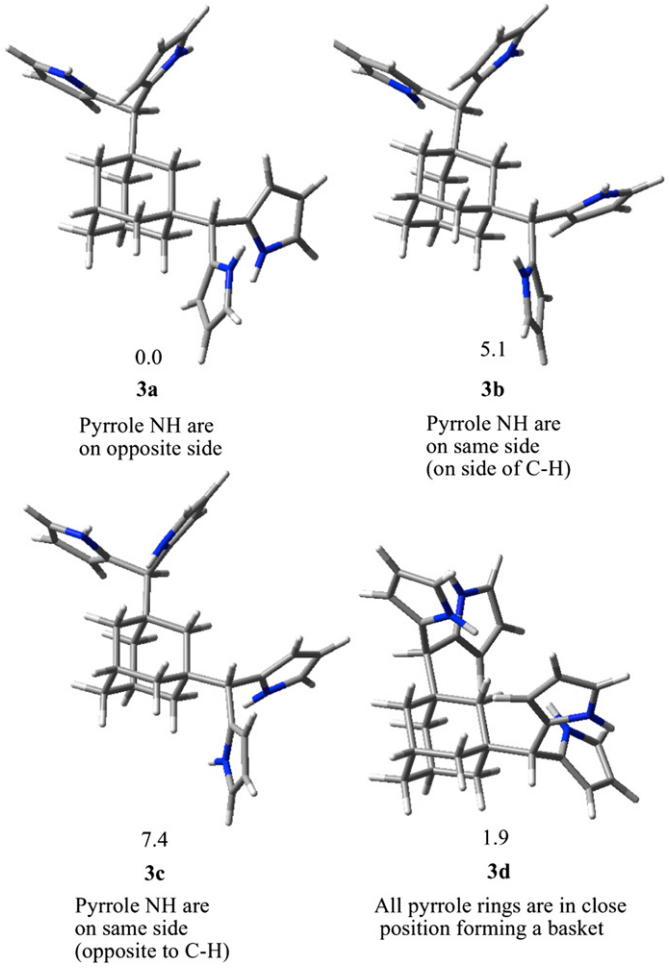

Figure 9. Semi-empirical PM3 optimized geometries and relative energies (kcal/mol) for various conformers of **3**. (Grey: carbon; blue: nitrogen; white: hydrogen).

the complex, F^- interacts with four pyrrole NH atoms (from two molecules). Unlike the 2:1 complexes of **2** with F^-, the *anti* configuration of **3**·F^- was found to be more stable than the *syn*. The binding energy for *anti*-**3**·F^- (2:1) was found to be higher compared to other binding complexes of **3**.

For AdD **4**, PM3 calculations showed a similar trend to **3**. However, ONIOM calculated binding energies show the preference towards the formation of **4**·F^- 1:2 over **4**·F^- 1:1 (Table 4). Furthermore, the calculation by both methods suggested that formation of *anti*-**4**·F^- (2:1) is energetically more favourable than 1:1 or

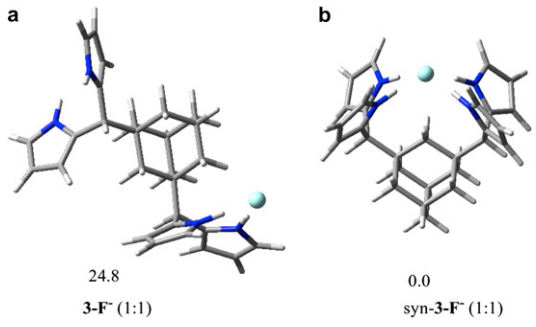

Figure 10. RHF/PM3 optimized geometries and relative energies (kcal/mol) of two possible conformers of the 1:1 complex of **3**·F^-: (a) **3**·F^- (1:1) and (b) *syn*-**3**·F^- (1:1). (Grey: carbon; blue: nitrogen; cyan: fluoride; white: hydrogen).

Table 5
PM3 calculated binding energies (kcal/mol) for receptor **1**–**4** interacting with fluoride ion in different ratio for **1**–**3** ($CHCl_3$) and **4** (in DMSO)

AdD·F.	(1:1)	*anti*-(2:1)	*syn*-(2:1)	(1:2)
1·**F**	−19.2	−37.5	−38.5	—
2·**F**	−16.9	−32.2	−36.6	—
3·**F**	−16.1 (−27.4)[a]	−34.0	−31.2	−26.2
4·**F**	−10.2	−20.5	−18.9	−19.9

[a] Fluoride ion interacted with all four nitrogens forming a basket like geometry [*syn*-**3**·F^- (1:1)].

1:2 (Table 4). This is however in contradiction with the observed results in solution. AdD **4** does not form 2:1 complex with F^- (vide supra).

It should be noted that different solvents ($CDCl_3$ and DMSO-d_6) were used in the experimental study to estimate the association of F^- with **3** and **4**. For **3**, when $CDCl_3$ was used, a 2:1 complex was observed, whereas the NMR titration performed in DMSO-d_6 indicated the presence of 1:1 and 2:1 complexes. Therefore, it is important to examine the role of the solvent in the complexation of F^- with **3** and **4**.

To account for the solvation effect, additional calculations were performed with PM3 optimized geometries of **1**–**4** with fluoride ion.[33] For receptors **1**–**3**, $CHCl_3$ was used as a solvent, and DMSO was considered for receptor **4**. The calculated energies with $CHCl_3$ show that the trends are similar to the gas phase data for **1**, **2** and **3** with F^- (Table 5). In all the three cases 2:1 complex is preferred over the 1:1 complex. Interestingly, the computed results showed that the 1:2 complex is comparable to 2:1 complex for receptor **4** (Table 5). The observed results indicated the formation of 1:2 complex for **4** with F^- ion in solution. There is nothing unusual in the intrinsic ability of **4** to change the complexation trend from **3**. The changes observed for **3** and **4** seems to be due to the difference in solvent polarity or the influence of solvent towards binding with the fluoride ions.

3. Conclusion

Adamantane-dipyrromethane receptors **1**–**4** form complexes with the following anions: $F^- \sim AcO^- > HSO_4^- >> H_2PO_4^- >>> Cl^-$, Br^- and NO_3^-. The stability constants of the complexes can be related to the basicity of the anion, the cavity shape around the anion, formed by the AdD receptor, and the accessibility of the proton donor groups for hydrogen bonding with anions. The most stable complexes are of 2:1 stoichiometry, and are observed with the most basic anions F^- and AcO^-. In these complexes two receptors with four proton donor groups are bonded to anion. Stability of the complex is also related to the anion size. Small F^- fits well in the cavity formed by two AdD receptor molecules forming four hydrogen bonds in tetrahedral fashion. Larger Cl^- cannot fit well in such a cavity, and in the solid state, a 2:1 complex with four coplanar hydrogen bonds is formed, whereas in the solution 1:1 complex occurred. The binding of the other anions is much weaker due to the lower basicity, larger size and larger dispersion of the charge in these anions. Therefore, in the dynamic solution system, less-flexibile AdD receptors form only weak 1:1 complexes with Cl^-, Br^-, NO_3^-, HSO_4^-, and $H_2PO_4^-$. The calculated binding energies for the AdD complexes with F^- reveal the prevalence for the formation of 2:1 complexes wherein the binding with four hydrogen bonds is accomplished. The gas phase calculations for the AdD derivatives **3** and **4**, which principally have two binding sites, also indicated preference for the formation of 2:1 complexes, rather than 1:1 or 1:2. The observed formation of the 1:1 and 1:2 stoichiometry with **4**, on the other hand, could be ascribed only to the difference of solvating ability of DMSO.

The information of the anion coordination presented in this study is of significant value in the design of new receptors that will be characterised by better binding activity and selectivity.

4. Experimental section

4.1. General

^{1}H and ^{13}C NMR spectra were recorded on a Spectrometer at 300 or 600 MHz. All NMR spectra were measured in $CDCl_3$ or DMSO-d_6 using tetramethylsilane as a reference. High-resolution mass spectra (HRMS) were measured on an FTMS 2001 DD using electron impact ionisation mode. Melting points were obtained using an Original Kofler apparatus and are uncorrected. Silica gel (0.05–0.2 mm) was used for chromatographic purifications. Solvents were purified by distillation. Adamantane-1-carbaldehyde (**6**),[34] adamantane-2-one (**7**),[35] adamantane-1,3-dicarbaldehyde (**8**)[36] and adamantane-2,6-dione (**9**)[37] were prepared according to the procedure described in the literature.

4.2. General procedure for preparation of the receptors 1–4

In a two neck flask under a stream of nitrogen one equivalent of carbaldehyde/ketone **6**–**9** in 40 equiv of pyrrole was dissolved. By use of a syringe, to the reaction mixture was added 0.1 equiv of TFA and the mixture was stirred at rt, while the progress of the reaction was followed by TLC using CH_2Cl_2 as an eluent. Upon the disappearance of the starting carbaldehyde/ketone, the reaction was quenched by the addition of an aqueous solution of NaOH (0.1 M, ~20 mL). To the mixture CH_2Cl_2 (20 mL) was added and the layers were separated. The aqueous layer was extracted two more times using CH_2Cl_2 (2×20 mL) organic extracts were washed with water (20 mL), collected and dried over anhydrous $MgSO_4$. After filtration, the solvent was evaporated on a rotary evaporator and the excess of pyrrole removed from the residue by a distillation under reduced pressure. The obtained dark residue was chromatographed on a column filled with silica gel using CH_2Cl_2 (or CH_2Cl_2/diethyl–ether mixture) as an eluent.

*4.2.1. 1-Di(pyrrole-2-yl)methyladamantane (**1**).* Obtained by reacting adamantane-1-carbaldehyde (**6**, 236 mg, 1.44 mmol) with pyrrole (3.89 g, 58 mmol, 4.0 mL) in the presence of TFA (10 μL, 0.14 mmol). After stirring over 1 h at rt the reaction was quenched and worked-up following the general procedure. After chromatography reaction furnished 207 mg (51%) of product **1** in the form of colourless crystals, which were further purified by recrystallisation from benzene/hexane mixture to remove the traces of unreacted pyrrole. Colourless crystals, mp 168–169 °C; ^{1}H NMR ($CDCl_3$, 600 MHz) δ 1.49–1.61 (m, 12H), 1.89 (br.s, 3H), 3.50 (s, 1H), 6.03–6.13 (m, 4H), 6.55–6.60 (m, 2H), 7.90 (br.s, 2H); ^{13}C NMR ($CDCl_3$, 150 MHz) δ 28.6 (d, 3C), 36.7 (t, 3C), 36.9 (s, 1C), 40.4 (t, 3C), 51.4 (d, 1C), 106.5 (d, 2C), 108.2 (d, 2C), 115.7 (d, 2C), 130.1 (s, 2C); IR (KBr) 3369 (s), 2927 (m), 2903 (m), 2864 (m) cm^{-1}; MS *m*/*z* (%): 279 (100, M−H$^+$); HRMS, calculated for $C_{19}H_{23}N_2$ 279.1861; observed 279.1859.

*4.2.2. 2,2-Di(pyrrole-2-yl)adamantane (**2**).* Obtained by reacting adamantane-2-one (**7**, 250 mg, 1.66 mmol) with pyrrole (4.47 g, 66 mmol, 4.6 mL) in the presence of TFA (13 μL, 0.17 mmol). After stirring over 1.5 h at rt the reaction was quenched and worked-up following the general procedure. After chromatography reaction furnished 143 mg of product **2** in the form of colourless crystals, which were further purified by rechromatography to yield 128 mg (29%). Colourless crystals, mp 183.4–185.2 °C; ^{1}H NMR ($CDCl_3$, 300 MHz) δ 1.69–1.87 (m, 8H), 2.16–2.26 (m, 4H), 2.64 (br.s, 2H), 6.04–6.07 (m, 4H), 6.56–6.58 (m, 2H), 7.78 (br s, 2H); ^{13}C NMR ($CDCl_3$, 75 MHz) δ 27.3 (d, 2C), 33.6 (t, 4C), 33.9 (d, 2C), 38.1 (t, 1C), 45.0 (s, 1C), 103.9 (d, 2C), 107.3 (d, 2C), 116.1 (d, 2C), 137.9 (s, 2C); IR (KBr) 3382 (s), 3097 (w), 2950 (m), 2924 (m), 2890 (m), 2894 (m), 1107 (m), 1028 (m), 787 (m), 727 (s) cm^{-1}; MS *m*/*z* (%): 265 (100, M−H$^+$); HRMS, calculated for $C_{18}H_{21}N_2$ 265.1705; observed 265.1706; Anal. Calcd. For $C_{18}H_{22}N_2$: C, 81.16; H, 8.32; N, 10.52. Found C, 81.17; H, 7.60; N, 10.71.

*4.2.3. 1,3-Bis[di(pyrrole-2-yl)methyl]adamantane (**3**).* Obtained by reacting adamantane-1,3-dicarbaldehyde (**8**, 244 mg, 1.27 mmol) with pyrrole (6.82 g, 102 mmol, 7.05 mL) in the presence of TFA (9.4 μL, 0.12 mmol). After stirring over 1 h at rt the reaction was quenched and worked-up following the general procedure. After chromatography (eluting with CH_2Cl_2 and by increasing polarity by the addition of diethyl-ether, up to 20%) reaction furnished 200 mg (37%) of product **3** in the form of colourless crystals, which were further purified by recrystallisation from the benzene/hexane mixture and dried on high vacuum. Colourless crystals, mp 110–112 °C; ^{1}H NMR ($CDCl_3$, 300 MHz) δ 1.55–1.38 (m, 12H), 1.96–2.02 (m, 2H), 3.55 (br.s, 2H), 6.00–6.19 (8H), 6.58–6.65 (m, 4H), 7.92 (br.s, 4H); ^{13}C NMR ($CDCl_3$, 75 MHz) δ 28.9 (d, 2C), 35.9 (t, 1C), 37.8 (d, 2C), 39.3 (t, 4C), 43.9 (s, 2C), 50.9 (d, 2C), 106.5 (d, 4C), 108.2 (d, 4C), 115.8 (d, 4C), 129.9 (s, 2C); IR (KBr) 3382 (s), 2901 (s), 2847 (m), 720 (s) cm^{-1}; MS *m*/*z* (%): 423 (100, M−H$^+$); HRMS, calculated for $C_{28}H_{31}N_4$ 423.2549; observed 423.2542.

*4.2.4. 2,2,6,6-Tetra(pyrrole-2-yl)adamantane (**4**).* Obtained by reacting adamantane-2,6-dione (**9**, 200 mg, 1.2 mmol) with pyrrole (6.44 g, 96 mmol, 6.6 mL) in the presence of TFA (9 μL, 0.12 mmol). After stirring over 1.5 h at rt the reaction was quenched and worked-up following the general procedure. After chromatography (eluting with CH_2Cl_2 and by increasing polarity by the addition of diethyl-ether, up to 20%) reaction furnished 75 mg (15%) of crude product **4** in the form of colourless crystals, which were further purified by recrystallization. Colourless crystals, decomposition above 215 °C; ^{1}H NMR (DMSO-d_6, 300 MHz) δ 1.83–1.95 (m, 8H), 2.63–2.72 (br s, 4H), 5.73–5.86 (m, 8H), 6.42–6.50 (m, 4H), 10.09 (br s, 4H); ^{13}C NMR (DMSO-d_6, 75 MHz) δ 29.2 (t, 4C), 31.2 (d, 4C), 44.3 (s, 2C), 103.7 (d, 4C), 106.5 (d, 4C), 115.2 (d, 4C), 138.2 (s, 4C); IR (KBr) 3409 (s), 3379 (s), 2959 (m), 2925 (m), 2899 (m), 2861 (m), 720 (s) cm^{-1}; MS *m*/*z* (%): 395 (75, M−H$^+$), 328 (100); HRMS, calculated for $C_{26}H_{27}N_4$ 395.2236; observed 395.2236.

4.3. ^{1}H NMR titrations

Typical proton NMR experiment was carried out in such a way that to a 0.5 mL of the $CDCl_3$ solution of **1**–**3** or **5** was added a solution of Bu_4NF (1 M in THF, containing <wt 5% H_2O) or Bu_4NCl, Bu_4NBr, Bu_4NHSO_4, $Bu_4NH_2PO_4$, Bu_4NOAc, Bu_4NNO_3 (~0.5 M in $CDCl_3$). In the case of **4** the titration was performed in DMSO-d_6 and anions were added as $CDCl_3$ solutions, except in the case of Bu_4NF, which was added as 1 M solution in THF. The concentration of the **1**–**4** or **5** in the NMR experiment was typically 0.05 M. The concentrations of the anions ranged from 0.01–0.1 M, reaching the maximal ratio of anion–AdD=3:1. After each addition, NMR spectra were recorded. As mentioned above association constants were determined by fitting the dependence of the chemical shift of the NH signal ($\Delta\delta$) to the anion concentration, using EQNMR program[17] (examples of the fittings are shown in Supplementary data, Figs. 1S–7S).

4.4. Crystallography

Single crystals of compound **2** and complexes of **1** and **2** with various anions were obtained by slow evaporation of acetonitrile/hexane (~1:1) solutions of the receptors and appropriate salt at the

4 °C. Single crystal of the complex of **4** with TBAF was grown from the DMSO-d_6 in the NMR tube at the room temperature. Complex of **2** with TBACl was obtained by vapour diffusion of ethanol into a CH_2Cl_2 solution containing the salt and ligand at the 4 °C. Single crystals **4**·F^- and **2**·F^- were measured on an Enraf–Nonius CAD-4 diffractometer using a graphite monocromated CuKα radiation at room temperature. Three standard reflections were measured each 120 min as intensity control. **2**, **2**·Ac^-, **2**·Cl^- and **1**·F^- were measured on an Oxford Diffraction Xcalibur Nova R (CCD detector, microfocus Cu tube) at room temperature. Program packages CrysAlis PRO[38] and XCAD-4[39] were used for data reduction. The structures were solved using SHELXS97[40] and refined with SHELXL97.[40] The models were refined using the full-matrix least squares refinement; all non-hydrogen atoms were refined anisotropically. Hydrogen atoms were located from difference Fourier maps whenever possible; otherwise they were treated as constrained entities, using the command AFIX in SHELXL97.[40] Molecular geometry calculations were performed by PLATON,[41] and molecular graphics were prepared using ORTEP-3,[42] and CCDC-Mercury.[43] Crystallographic and refinement data for the structures reported in this paper are shown in Supplementary data. Crystallographic data for the structural analysis has been deposited with the Cambridge Crystallographic Data Centre, CCDC 747952–747957. Copies of the data can be obtained, free of charge, on application to CCDC, 12 Union Road, Cambridge, CB2 1EZ, UK (fax: +44 1223 336033 or e-mail: deposit@ccdc.ac.uk).

4.5. Computational methods

All geometries were fully optimized in gas phase with semi-empirical PM3 method.[30] The harmonic frequency analysis has also been performed for stationary points to confirm minima at the same level of theory. For more accurate predictions of binding energies employing PM3 calculated geometries, single point calculations were performed using ONIOM method at (B3LYP/6-31+G*:PM3) level.[32] Solvent calculations were performed with PM3 optimised geometries using polarized continuum salvation model (PCM) at same level of theory.[33] Chloroform was used as a solvent for receptors **1**–**3** and their complexes with F^-, however, DMSO was used for receptor **4** and their complexes with F^-. All calculations were carried out with the Gaussian 03.[44]

Acknowledgements

The financing from the Ministry of Science, Education and Sports of the Republic of Croatia (grant no. 098-0982933-2911; 098-1191344-2943 and India-Croatia bilateral project 910-08105-01/243) is gratefully acknowledged. We thank Prof. M.J. Hynes for the EQNMR program and J. Alešković for the help to apply the program. We also thank S. Roca for recording NMR spectra. MKK thanks UGC, New Delhi, India for awarding junior research fellowship.

Supplementary data

Supplementary data associated with this article can be found, in the online version, at doi:10.1016/j.tet.2010.01.018.

References and notes

1. (a) Bianchi, A.; Bowman-James, K.; Garcia-España, E. *Supramolecular Chemistry of Anions*; Wiley-VCH: New York, NY, 1997; (b) Beer, P. D.; Gale, P. A. *Angew. Chem., Int. Ed.* **2001**, *40*, 486–516; (c) Gale, P. A. *Coord. Chem. Rev.* **2003**, *240* 1; (d) Bowman-James, K. *Acc. Chem. Res.* **2005**, *38*, 671–678; (e) Top. Curr. Chem. 2005, Vol. 255 (Ed.: I. Stibor). (f) Gale, P. A. *Coord. Chem. Rev.* **2006**, *250* 2917; (g) Caltagirone, C.; Gale, P. A. *Chem. Soc. Rev.* **2009**, *38*, 520–563.
2. (a) Schmidtchen, F. P.; Berger, M. *Chem. Rev.* **1997**, *97*, 1609–1646; (b) Schmidtchen, F.P., in Top. Curr. Chem. 2005, Vol. 255, (Ed.: I. Stibor) 1–29; (c) Schmidtchen, F. P. *Coord. Chem. Rev.* **2006**, *250*, 2918–2928; (d) Gale, P. A. *Acc. Chem. Res.* **2006**, *39*, 465–475; (e) Katayev, E. A.; Ustynyuk, Y. A.; Sessler, J. L. *Coord. Chem. Rev.* **2006**, *250*, 3004–3037; (f) Kang, S. O.; Begum, A.; Bowman-James, K. *Angew. Chem., Int. Ed.* **2006**, *45*, 7882–7894.
3. (a) de Silva, A. P.; Gunaratne, H. Q. N.; Gunnlaugsson, T.; Huxley, A. J. M.; McCoy, C. P.; Rademacher, J. T.; Rice, T. E. *Chem. Rev.* **1997**, *97*, 1515–1566; (b) Martínez-Máñez, R.; Sancenón, F. *Chem. Rev.* **2003**, *103*, 4419–4476; (c) Callan, J. F.; de Silva, A. P.; Magri, D. C. *Tetrahedron* **2005**, *61*, 8551–8558; (d) Gunnlaugsson, T.; Glynn, M.; Tocci, G. M.; Kruger, P. E.; Pfeffer, F. M. *Coord. Chem. Rev.* **2006**, *250*, 3094–3117.
4. (a) Buhlmann, P.; Pretsch, E.; Bakker, E. *Chem. Rev.* **1998**, *98*, 1593–1687; (b) Davis, F.; Collyer, S.D.; Higson, S.P.J., in Top. Curr. Chem. 2005, Vol. 255, (Ed.: I. Stibor), 97–124.
5. Sasson, Y.; Neumann, R. In *Handbook of Phase Transfer Catalysis*; Sasson, Y., Neumann, R., Eds.; Chapman & Hall: London, 1997; pp 510–546.
6. (a) Lankshear, M. D.; Beer, P. D. *Coord. Chem. Rev.* **2006**, *250*, 3142–3160; (b) Gimeno, N.; Vilar, R. *Coord. Chem. Rev.* **2006**, *250*, 3161–3189.
7. (a) Gale, P. A.; Sessler, J. L.; Král, V.; Lynch, V. *J. Am. Chem. Soc.* **1996**, *118*, 5140–5141; (b) Gale, P. A.; Sessler, J. L.; Král, V. *Chem. Commun.* **1998**, 1–8; (c) Sessler, J. L.; Tvermoes, N. A.; Davis, J.; Anzenbacher, P., Jr.; Jursíková, K.; Sato, W.; Seidel, D.; Lynch, V.; Black, C. B.; Try, A.; Andrioletti, B.; Hemmi, G.; Mody, T. D.; Magda, D. J.; Král, V. *Pure Appl. Chem.* **1999**, *71*, 2009–2018; (d) Gale, P. A.; Anzenbacher, P., Jr.; Sessler, J. L. *Coord. Chem. Rev.* **2001**, *222*, 57–102; (e) Sessler, J. L.; Davis, J. M. *Acc. Chem. Res.* **2001**, *34*, 989–997; (f) Cafeo, G.; Kohnke, F. H.; La Torre, G. L.; Parisi, M. F.; Pistone Nascone, R.; White, A. J. P.; Williams, D. J. *Chem.— Eur. J.* **2002**, *8*, 3148–3156; (g) Sessler, J. L.; Camiolo, S.; Gale, P. A. *Coord. Chem. Rev.* **2003**, *240*, 17–55; (h) Sessler, J. L.; Davis, J. M.; Král, V.; Kimbrough, T.; Lynch, V. *Org. Biomol. Chem.* **2003**, *1*, 4113–4123; (i) Nishiyabu, R.; Anzenbacher, P., Jr. *J. Am. Chem. Soc.* **2005**, *127*, 8270–8271; (j) Sessler, J. L.; An, D.; Cho, W.-S.; Lynch, V.; Marquez, M. *Chem.— Eur. J.* **2005**, *11*, 2001–2011; (k) Blas, J. R.; Lopez-Bes, J. M.; Marquez, M.; Sessler, J. L.; Luque, F. J.; Orozco, M. *Chem.— Eur. J.* **2007**, *13*, 1108–1116.
8. (a) Gale, P. A.; Camiolo, S.; Chapman, C. P.; Light, M. E.; Hursthouse, M. B. *Tetrahedron Lett.* **2001**, *42*, 5095–5097; (b) Gale, P. A.; Camiolo, S.; Tizzard, G. J.; Chapman, C. P.; Light, M. E.; Coles, S. J.; Hursthouse, M. B. *J. Org. Chem.* **2001**, *66*, 7849–7853; (c) Navakhun, K.; Gale, P. A.; Camiolo, S.; Light, M. E.; Hursthouse, M. B. *Chem. Commun.* **2002**, 2084–2085; (d) Vega, I. E. D.; Gale, P. A.; Hursthouse, M. B.; Light, M. E. *Org. Biomol. Chem.* **2004**, *2*, 2935–2941; (e) Gale, P. A. *Chem. Commun.* **2005**, 3761–3772; (f) Vega, I. E. D.; Camiolo, S.; Gale, P. A.; Hursthouse, M. B.; Light, M. E. *Chem. Commun.* **2003**, 1696–1698.
9. (a) Schmuck, C.; Geiger, L. *J. Am. Chem. Soc.* **2004**, *126*, 8898–8899; (b) Schmuck, C.; Heil, M. *ChemBioChem* **2003**, *4*, 1232–1238; (c) Schmuck, C.; Bickert, V. *Org. Lett.* **2003**, *5*, 4579–4581; (d) Schmuck, C.; Dudaczek, J. *Tetrahedron Lett.* **2005**, *46*, 7101–7105.
10. (a) Anzenbacher, P., Jr.; Try, A. C.; Miyaji, H.; Jursikova, K.; Lynch, V. M.; Marquez, M.; Sessler, J. L. *J. Am. Chem. Soc.* **2000**, *122*, 10268–10272; (b) Sessler, J. L.; Black, C. B.; Andrioletti, B.; Try, A. C.; Ruiperez, C. *J. Am. Chem. Soc.* **1999**, *121*, 10438–10439; (c) Mizuno, T.; Wei, W. H.; Eller, L. R.; Sessler, J. L. *J. Am. Chem. Soc.* **2002**, *124*, 1134–1135; (d) Sessler, J. L.; Hiromistu, M.; Mizuno, T.; Lynch, V. M.; Furuta, H. *Chem. Commun.* **2002**, 862–863.
11. (a) Lindsey, J.S.; Savithri, D.; Joyder, K.l., Masahiko, T. US 2005/0038262 A1, Feb 17 2005. (b) Litter, B. J.; Miller, M. A.; Hung, C.-H.; Wagner, R. W.; O'Shea, D. F.; Boyle, P. D.; Lindsey, J. S. *J. Org. Chem.* **1999**, *64*, 1391–1396; (c) Wilson, R. M.; Hengge, A. *J. Org. Chem.* **1987**, *52*, 2699–2707.
12. (a) Pfeffer, F. M.; Gunnlaugsson, T.; Jensen, P.; Kruger, P. E. *Org. Lett.* **2005**, *7*, 5357–5360; (b) Lowe, A. J.; Dyson, G. A.; Pfeffer, F. M. *Org. Biomol. Chem.* **2007**, *5*, 1343–1346; (c) Pfeffer, F. M.; Kruger, P. E.; Gunnlaugsonn, T. *Org. Biomol. Chem.* **2007**, *5*, 1894–1902.
13. (a) Basarić, N.; Renić, M.; Majerski, K., HR patent P20070111A, 2007: (b) Basarić, N.; Renić, M.; Majerski, K., PCT HR2008/000008, 2008.
14. Renić, M.; Basarić, N.; Mlinarić-Majerski, K. *Tetrahedron Lett.* **2007**, *48*, 7873–7877.
15. (a) Aakeröy, C. B.; Seddon, K. R. *Chem. Soc. Rev.* **1993**, *22*, 397–407; (b) Custelcean, R. *Chem. Commun.* **2008**, 295–307.
16. (a) Sessler, J. L.; Gross, D. E.; Cho, W.-S.; Lynch, V. M.; Schmidtchen, F. P.; Bates, G. W.; Light, M. E.; Gale, P. A. *J. Am. Chem. Soc.* **2006**, *128*, 12281–12288; (b) Amendola, V.; Esteban-Gómez, D.; Fabbrizzi, L.; Licchelli, M. *Acc. Chem. Res.* **2006**, *39*, 343–353.
17. Hynes, M. J. *J. Chem. Soc., Dalton Trans.* **1993**, 311–312.
18. (a) Connors, K. A. *Binding Constants*; John Wiley & Sons: New York, NY, 1987; (b) Fielding, L. *Tetrahedron* **2000**, *56*, 6151–6170.
19. For deprotonation of some pyrrole derivatives see: (a) Camiolo, S.; Gale, P. A.; Hursthouse, M. B.; Light, M. E.; Shi, A. J. *Chem. Commun.* **2002**, 758–759; (b) Evans, L. S.; Gale, P. A.; Light, M. E.; Quesada, R. *Chem. Commun.* **2006**, 965–967; (c) Lin, C.; Simov, V.; Drueckhammer, D. G. *J. Org. Chem.* **2007**, *72*, 1742–1746.
20. Jeffrey, G. A. *An Introduction to Hydrogen Bonding*; Oxford University Press: Oxford, 1997.
21. Bernstein, J.; Davies, R. E.; Shimoni, L.; Chang, N.-L. *Angew. Chem., Int. Ed. Engl.* **1995**, *34*, 1555–1573.
22. Allen, F. H. *Acta Cryst. B* **2002**, *58*, 380–388.
23. (a) Sessler, J. L.; Eller, L. R.; Cho, W.-S.; Nicolaou, S.; Aguilar, A.; Lee, J. T.; Lynch, V. M.; Magda, D. J. *Angew. Chem., Int. Ed.* **2005**, *44*, 5989–5992; (b) Sessler, J. L.; Weghorn, S. J.; Lynch, V.; Fransson, K. *J. Chem. Soc., Chem. Commun.* **1994**, 1289–1290.

24. Gale, P. A.; Light, M. E.; McNally, B.; Navakhun, K.; Sliwinski, K. E.; Smith, B. D. *Chem. Commun.* **2005**, 3773–3775.
25. Brooks, S. J.; Edwards, P. R.; Gale, P. A.; Light, M. E. *New J. Chem.* **2006**, *30*, 65–75.
26. Sessler, J. L.; Cyr, M. J.; Lynch, V.; McGhee, E.; Ibers, A. *J. Am. Chem. Soc.* **1990**, *112*, 2810–2813.
27. Sessler, J. L.; Cho, W.-S.; Gross, D. E.; Shriver, J. A.; Lynch, V. M.; Marquez, M. *J. Org. Chem.* **2005**, *70*, 5982–5986.
28. Sessler, J. L.; An, D.; Cho, W.-S.; Lynch, V.; Yoon, D.-W.; Hong, S.-J.; Lee, C.-H. *J. Org. Chem.* **2005**, *70*, 1511–1517.
29. Brooks, S. J.; Gale, P. A.; Light, M. E. *Chem. Commun.* **2005**, 4696–4698.
30. (a) Stewart, J. J. P. *J. Comput. Chem.* **1989**, *10*, 209–220; (b) Stewart, J. J. P. *J. Comp. Chem.* **1989**, *10*, 221–264.
31. (a) Becke, A. D. *J. Chem. Phys.* **1993**, *98*, 5648–5652; (b) Lee, C.; Yang, W.; Parr, R. G. *Phys. Rev. B* **1988**, *37*, 785–789.
32. (a) Maseras, F.; Morokuma, K. *J. Comp. Chem.* **1995**, *16*, 1170–1179; (b) Humbel, S.; Sieber, S.; Morokuma, K. *J. Chem. Phys.* **1996**, *105*, 1959–1967.
33. (a) Tomasi, J.; Persico, M. *Chem. Rev.* **1994**, *94*, 2027–2094; (b) Cossi, M.; Barone, V.; Cammi, R.; Tomasi, J. *Chem. Phys. Lett.* **1996**, *255*, 327–335; (c) Barone, V.; Cossi, M.; Tomasi, J. *J. Chem. Phys.* **1997**, *107*, 3210–3221; (d) Barone, V.; Cossi, M.; Tomasi, J. *J. Comput. Chem.* **1998**, *19*, 404–417.
34. Bott, K. *Angew. Chem.* **1968**, *80*, 970.
35. Geluck, H. W.; Keiser, V. G. *Org. Synth. Coll.* **1988**, *6*, 48–50.
36. Klaić, L.; Alešković, M.; Veljković, J.; Mlinarić-Majerski, K. *J. Phys. Org. Chem.* **2008**, *21*, 299–305.
37. Geluk, H. W.; Schlatmann, J. L. M. A. *RECUEIL* **1971**, *90*, 516–520.
38. *CrysAlis PRO*; Oxford Diffraction Ltd.: U.K., 2007.
39. Harms, K.; Wocadlo, S. *XCAD-4, Program for Processing CAD4 Diffractometer Data*; University of Marburg: Germany, 1995.
40. Sheldrick, G. M. *Acta Crystallogr. A* **2008**, *A64*, 112–122.
41. Spek, A. L. *J. Appl. Crystallogr.* **2003**, *36*, 7–13.
42. Farrugia, L. J. *J. Appl. Crystallogr.* **1997**, *30*, 565.
43. Macrae, C. F.; Edgington, P. R.; McCabe, P.; Pidcock, E.; Shields, G. P.; Taylor, R.; Towler, M.; ven de Streek, J. *J. Appl. Crystallogr.* **2006**, *39*, 453–457.
44. Frisch, M. J.; Trucks, G. W.; Schlegel, H. B.; Scuseria, G. E.; Robb, M. A.; Cheeseman, J. R.; Montgomery, J. A., Jr.; Vreven, T.; Kudin, K. N.; Burant, J. C.; Millam, J. M.; Iyengar, S. S.; Tomasi, J.; Barone, V.; Mennucci, B.; Cossi, M.; Scalmani, G.; Rega, N.; Petersson, G. A.; Nakatsuji, H.; Hada, M.; Ehara, M.; Toyota, K.; Fukuda, R.; Hasegawa, J.; Ishida, M.; Nakajima, T.; Honda, Y.; Kitao, O.; Nakai, H.; Klene, M.; Li, X.; Knox, J. E.; Hratchian, H. P.; Cross, J. B.; Bakken, V.; Adamo, C.; Jaramillo, J.; Gomperts, R.; Stratmann, R. E.; Yazyev, O.; Austin, A. J.; Cammi, R.; Pomelli, C.; Ochterski, J. W.; Ayala, P. Y.; Morokuma, K.; Voth, G. A.; Salvador, P.; Dannenberg, J. J.; Zakrzewski, V. G.; Dapprich, S.; Daniels, A. D.; Strain, M. C.; Farkas, O.; Malick, D. K.; Rabuck, A. D.; Raghavachari, K.; Foresman, J. B.; Ortiz, J. V.; Cui, Q.; Baboul, A. G.; Clifford, S.; Cioslowski, J.; Stefanov, B. B.; Liu, G.; Liashenko, A.; Piskorz, P.; Komaromi, I.; Martin, R. L.; Fox, D. J.; Keith, T.; Al-Laham, M. A.; Peng, C. Y.; Nanayakkara, A.; Challacombe, M.; Gill, B.; Johnson, P. M. W.; Chen, W.; Wong, M. W.; Gonzalez, C.; Pople, J. A. *Gaussian 03, Revision E.01*; Gaussian,: Wallingford, CT, 2004.